Pure appl. geophys. 161 (2004) 429–451
0033–4553/04/020429–23
DOI 10.1007/s00024-003-2447-4

Pure and Applied Geophysics

Simulation of the Urban Heat Island Phenomenon in Mediterranean Climates

G. Mihalakakou[1], M. Santamouris[1], N. Papanikolaou[1], C. Cartalis[1], and A. Tsangrassoulis[1]

Abstract—An intelligent "data-driven" method is used in the present study for investigating, analyzing and quantifying the urban heat island phenomenon in the major Athens region where hourly ambient air-temperature data are recorded at twenty-three stations. The heat island phenomenon has a serious impact on the energy consumption of buildings, increases smog production, while contributing to an increasing emission of pollutants from power plants, including sulfur dioxide, carbon monoxide, nitrous oxides and suspended particulates.

The intelligent method is an artificial neural network approach in which the urban heat island intensity at day and nighttime are estimated using as inputs several climatic parameters. Various neural network architectures are designed and trained for the output estimation, which is the daytime and nighttime urban heat island intensity at each station for a two-year time period. The results are tested with extensive sets of non-training measurements and it is found that they correspond well with the actual values. Furthermore, the influence of several input climatic parameters measured at each station, such as solar radiation, daytime and nighttime air temperature, and maximum daily air temperature, on the urban heat island intensity fluctuations is investigated and analyzed separately for the day and nighttime period. From this investigation it is shown that heat island intensity is mainly influenced by urbanization factors. A sensitivity investigation has been performed, based on neural network techniques, in order to adequately quantify the impact of the above input parameters on the urban heat island phenomenon.

Key words: Heat island phenomenon, heat island intensity, neural networks.

1. Introduction

Air temperatures in densely built urban areas are higher than those of the surrounding rural country. This phenomenon, which is widely known as "urban heat island," is regarded as the most representative and documented manifestation of climatic modification. Heat island is present in every town and city and is the most obvious climatic indication of urbanization (Landsberg, 1981).

Increased industrialization and urbanization in recent years have affected dramatically the number of urban buildings with major effects on the energy consumption of this sector. Urban areas without a high climatic quality use more

[1] Laboratory of Meteorology, Division of Applied Physics, Department of Physics, University of Athens, Athens, Greece. E-mail: pmihalak@cc.uoa.gr

energy for air conditioning in summer and even more electricity for lighting. Moreover, discomfort and inconvenience to the urban population due to high temperatures, wind tunnel effects in streets and unusual wind turbulence due to wrongly designed high rise buildings is a very common phenomenon (SANTAMOURIS *et al.*, 2001).

Temperature distribution in urban areas is highly affected by the urban radiation balance. Solar radiation incident on urban surfaces is absorbed and then transformed to sensible heat. Most of the solar radiation impinges on roofs, and the vertical walls of the buildings, and only a relatively small part reaches the ground level. Walls, roofs and the ground emit long wave radiation to the sky. The intensity of the emitted radiation depends on the view factor of the surface regarding the sky. Under urban conditions most of the sky dome viewed by walls and surfaces is blocked by other buildings, and thus the long wave radiant exchange does not really result in significant losses. The net balance between the solar gains and the heat loss by emitted long-wave radiation determines the thermal balance of urban areas, which are less efficient at achieving the balance and hence these areas require a higher temperature to achieve this balance. The urban heat island phenomenon may occur during day or nighttime periods and its patterns are strongly controlled by the unique characteristics of each urban area. It is usually developed during clear, calm evenings and nights and is normally a result of delayed cooling of the city compared to surrounding rural areas (BARRING *et al.*, 1985). Although the reasons for this phenomenon are rather complex, the major causes are the differences in the thermal structures between the urban and rural environments such as the polluted air of the city, the anthropogenic heat released by the urban pollution, the thermal characteristics of the urban fabric and the urban geometry (PARK, 1986; OKE *et al.*, 1991).

The heat island phenomenon can be quantified by the maximum difference between urban temperature and the background rural temperature, which is defined as the urban heat island intensity (OKE, 1987). Heat island intensity depends on the size, population and industrial development of the city, the topography and the surface materials, the general climate of the region and the momentary meteorological conditions.

The effect of meteorological parameters on urban heat island intensity, (UHI), was the subject of considerable research (JOHNSON *et al.*, 1991; MONTAVEZ *et al.*, 2000; MORRIS *et al.*, 2000). Various studies revealed that wind speed and cloud amount are very important factors that influence the development and intensity of the UHI, suggesting that UHI intensifies under cloudless sky and light wind conditions. The city of Athens is characterized by a strong heat island effect, mainly caused by accelerated industrialization and urbanization during recent years. This phenomenon is mainly influenced and affected by the atmospheric circulation which is responsible for the formation and evolution of the meteorological elements that can enforce or eliminate the phenomenon (MIHALAKAKOU *et al.*, 2001).

An intelligent method such as the neural network systems is designed in the current research for estimating the urban heat island intensity in various locations of a large urban area. Important climatological parameters such as solar radiation, diurnal and nocturnal air temperature, and maximum air temperature are used as inputs to the models. Artificial neural networks are computational systems which can be regarded as an attempt to simulate in a simpler way the structure and functions of the human brain (LI *et al.*, 1990; CICHOCKI and UNBEHAUEN, 1993). The main characteristic of neural network models is their capability of modeling complex nonlinear processes. They belong to the class of ''data-driven'' approaches instead of ''model-driven'' methods because the analysis and the results depend on the available data (CHAKRABORTY *et al.*, 1992). Relationships between variables, models, laws and predictions are constructed after building a machine which simulates the considered data. The process of constructing such a machine based on available data is addressed by certain algorithms like ''perceptron'' (ROSENBLATT, 1961) or ''backpropagation'' (RUMELHART *et al.*, 1986). Various researchers proposed neural networks learning algorithms for time series predictions and estimations as well as for several energy applications (HONDOU and SAWADA, 1994; DASH *et al.*, 1995; KALOGIROU *et al.*, 1997; MIHALAKAKOU *et al.*, 1998; SANTAMOURIS *et al.*, 1999a,b). Air temperature is a chaotic time series and certainly, it can be predicted and estimated using linear methods. There are various studies in which researchers present comparisons between the results of a neural network model and those of a linear autoregressive one (MIHALAKAKOU *et al.*, 1998). From the above-mentioned studies it was concluded that the neural network makes significantly better estimations than those of the autoregressive model. Linear models are incapable of capturing the nonlinear nature of air temperature time series. The main advantage of the neural network model is that it enables the user to approximate or reconstruct any nonlinear activation function, and therefore such a model is sufficiently flexible.

The objectives of the present study are primarily to examine in depth, using the neural network techniques, the influence of the input climatic parameters on the heat island fluctuations, thus providing a quantitative information on the dependence of the urban heat island phenomenon on various climatic elements such as air temperature and solar radiation. The second objective is to investigate the ability of neural network systems for estimating the nighttime and daytime urban heat island intensity at twenty-three experimental stations in Athens for a two-year time period, using as inputs substantial climatic parameters.

The paper is organized as follows: The experimental investigation of the heat island phenomenon in the major Athens region is presented in section 2. The neural network models description and the urban heat island intensity as a function of the main climatic parameters are presented in section 3 for the nighttime temperature fluctuations and in section 4 for the daytime. Finally a summary and the conclusions are given in section 5.

2. The Urban Heat Island Experiment in Athens

2.1. Brief Description of the Area and the Prevailing Climatic Conditions

The Greater Athens Area, (GAA), is situated on a small peninsula located on the southeastern edge of the Greek mainland (Fig 1). It is divided by high mountains in three main parts, which are connected by small openings. The central part is the Athens basin which covers an area of 450 km^2, with a population density of 8000 inhabitants per square kilometer, with the main axis orientated from SSW to NNE. Athens basin is surrounded by high mountains in the north (Parnitha, 1426 m), in the west (Egaleo, 458 m) and in the east (Hymettus, 1026 m and Penteli, 1107 m), while it is open to the sea from the south (Saronikos Gulf). The other parts of the Athens area are the Thriassion plain west of the Athens basin and the Mesogia plain in the east. There are only small openings through which the Athens basin communicates with these plains as well as the rest of Greek mainland. These openings play an important role in air mass exchange between the Athens basin and the Thriassion and Mesogia plains (ASIMAKOPOULOS *et al.*, 1992; HELMIS *et al.*, 1997).

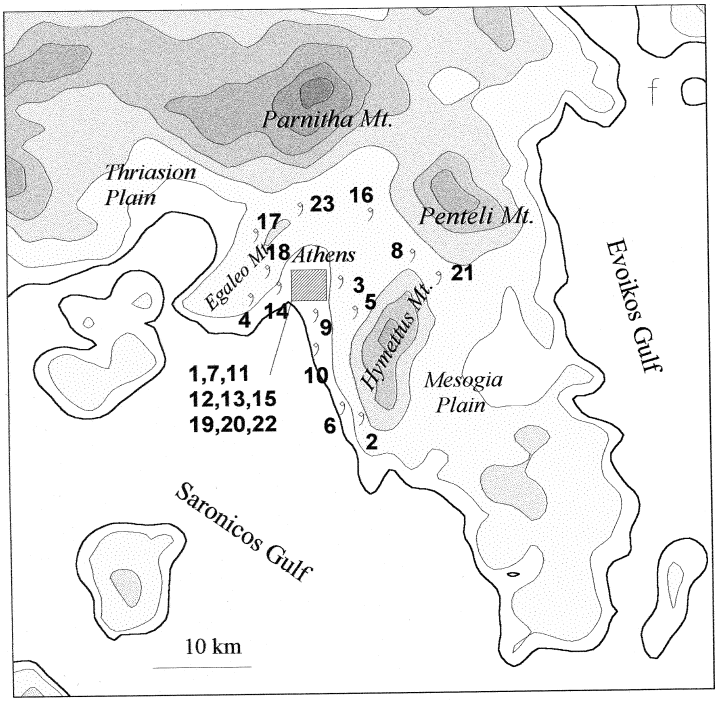

Figure 1
The locations of the 23 experimental stations.

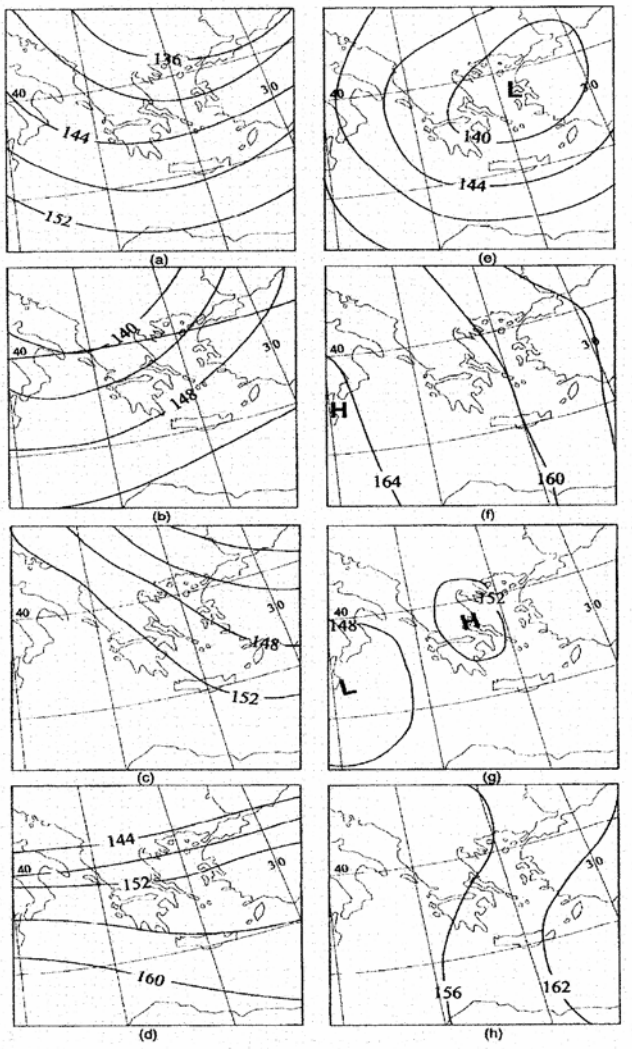

Figure 2
Schematic presentation of the eight synoptic categories over GAA.

A manual scheme for classifying the day-by-day 850-hPa atmospheric circulation over GAA was proposed and employed by KASSOMENOS *et al.* (1998). According to this study, the synoptic categories, illustrated in Figure 2, are the following (MIHALAKAKOU *et al.*, 2001):

1. Long-wave trough, characterized by intense winds, especially during the cold period of the year (Fig. 2a).
2. Southwesterly flow, characterized by a southwesterly flow which is usually very strong (Fig. 2b).

3. Northwesterly flow, characterized by strong cold air advection from the north or northwest (Fig. 2c).
4. Zonal flow, characterized by a westerly flow with considerably lower intensity in the warm period of the year (Fig. 2d).
5. Closed low, characterized by the presence of a closed low accompanied by intense winds, usually from the northern sector and rainfall (Fig. 2e).
6. High pressure ridge, characterized by a weak pressure gradient and weak, variable winds or calm conditions (Fig. 2f).
7. Closed anticyclone, characterized by the presence of a closed anticyclone that extends over the Greek area accompanied by weak winds from the southern or northern sector (Fig. 2g).
8. Category high-low, characterized by strengthening of the pressure gradient and strong northeasterlies that blow over the Aegean Sea and into the GAA (Fig. 2h).

The anticyclonic circulation prevails over the Athens area with maximum occurrence in January and June. A significant meteorological feature of the area is the predominance of high pressure systems combined with low pressure ones, resulting in rather complicated flow regimes, especially during July and August. Conditions of a cyclonic type seem to dominate in February and March while a south-westerly flow prevails in November and April.

The prevailing anticyclonic circulation in the Athens area favors the strong development of the heat island phenomenon.

2.2. Experimental Investigation

The Athens central region can be regarded as a special pilot study of the urban heat island effect caused by the accelerated industrialization and urbanization of recent years (SANTAMOURIS, 2001). The urban heat island phenomenon has been investigated using measurements from twenty-three experimental stations installed in the Athens urban and suburban region (Fig. 1). Hourly ambient air temperature and humidity values were recorded at the 23 stations for a time period of two years (1996 and 1997). The instrumentation used in the experiment was selected to satisfy several criteria such as acceptable cost, covering as many locations as possible, satisfactory performance according to the international meteorological standards, low maintenance, internal power supply and high data storage capacity. As the study had to cover the Athens basin, measurement points were selected with the following criteria:
a) to acquire information pertaining to the boundary conditions around the basin,
b) to study densely built areas with heavy traffic,
c) to study densely built areas with less traffic,
d) to study the conditions in green areas of the city center,
e) to study medium density built areas.

Therefore an attempt was made to select areas according to these criteria, that additionally are located on the north-south and east-west axes of the city. A brief

Table 1

Characteristics of the Experimental Stations

Station Number	Station Characteristics
1	Placed on a green hill at the center of Athens (altitude = 107 m). The area is characterized by low-building density and absence of traffic.
2	Placed in southeastern area of Athens near a mountain. The area is less populated with low traffic and medium building density.
3	Placed in the eastern area of Athens center. The area is densely populated with considerable traffic.
4	Placed in southwestern area of Athens. The area is less populated with low traffic while its vegetation is nearly negligible.
5	Placed in the eastern area of Athens near a mountain. The area is highly populated with considerable traffic.
6	Placed in the southern coastal area of Athens, very close to the airport. The area is characterized by very low traffic and by very few buildings.
7	Placed in the center of Athens. The area is densely populated with heavy traffic.
8	Placed in the northeastern area of Athens between two mountains. The area is characterized by increased building density and by heavy traffic.
9	Placed in the southern area of Athens center in a big avenue. The area is highly populated with heavy traffic.
10	Placed in the southern side of the previous avenue very close to the sea. The area is characterized by low building density and by heavy traffic.
11	Placed in the center of Athens in a pedestrian road. The area is very densely built and populated.
12	Placed in the center of Athens. The area is characterized by heavy traffic and by very dense population.
13	Placed in the center of Athens. Traffic and building density are very high.
14	Placed in the western area of Athens in a university campus characterized by a moderate vegetation.
15	Placed in the center of Athens. The area is very densely populated with considerable traffic.
16	Placed in the northern area of Athens. Traffic is very low and trees are scattered throughout the area.
17	Placed in the western limits of Athens basin in a football ground at the edge of a planted area. The area is characterized by very low traffic and building density.
18	Placed in the western area of Athens. Traffic is heavy while building density is very high.
19	Placed in the city center inside National Garden of Athens.
20	Placed in the Ancient Market of Athens. It is an area covered by bare soil and surrounded by trees.
21	Placed in the northeastern area of Athens in a suburb with increased traffic and average vegetation.
22	Placed in the center of Athens. The area is characterized by heavy traffic and large green spaces which consist of gardens and trees.
23	Placed very near the center of Athens in a big avenue. The area is not very densely built with an average street vegetation but its traffic is high.

description of each experimental station is presented in Table 1. Seven stations are placed in the central area of Athens, fifteen stations are placed in urban areas and in a radial configuration around Athens, while one station is placed in an almost

rural region, at the foot of a mountain, in order to be used as the reference station.

The instruments measuring the air temperature values are installed in buildings at a height approaching 5 m, while south orientation is selected for all thermometers. Miniature temperature data loggers equipped with a thermistor as a sensing element are used for measuring the hourly values of ambient air temperature at each experimental location. The technical characteristics of the utilized instruments are the following:

1. Data storage capacity: 7600 readings, for the measurement of hourly values, the instrument can operate for approximately 300 days.
2. Temperature range: −40 to 125 °C.
3. Accuracy of the sensors: ±0.2 °C.
4. Logger resolution: 0.5 °C.

At each station, approximating the Stevenson screen, white wooden boxes with lateral slots were constructed for the instruments' protection from solar radiation and rain. The boxes with the instruments were equipped with openings which offered natural ventilation. The temperature sensors were calibrated using an accurate liquid bath.

3. Fluctuations of the Nighttime Urban Heat Island Intensity

3.1. Modeling the Nighttime Heat Island Intensity

Artificial neural networks are computing systems which attempt to simulate the structure and function of biological neurons. How the inter-neuron connections are arranged and the nature of the connections determine the structure of a network (PHAM and LIU, 1995).

The estimation problem using neural network models can be separated into three successive steps or subproblems:

- Model building or neural network architecture.
- The learning or training procedure.
- The testing or diagnostic checking.

In the present research a multiple-layered network, based on backpropagation learning algorithm, is designed for the urban heat island intensity estimation at nighttime for every location. For this reason, a neural network model is built separately for each of the experimental stations. The selected neural network architecture consists of one hidden layer of 16 to 27 log-sigmoid neurons followed by an output layer of one linear neuron (MIHALAKAKOU *et al.*, 1998). Learning is achieved using the backpropagation algorithm of RUMELHART *et al.* (1986) to train the network.

The network is trained over a certain part of the climatic data and once training is completed, the network is tested over the remaining data.

The neural models are designed and trained for the estimation of the stations nighttime heat island intensity, ($\Delta T_{\max,n}$ in °C), which is considered to be the maximum difference between the ambient air temperature measured at an urban station and the one measured at a reference, during the nighttime and for a two-year time period (1996 and 1997).

$$\Delta T_{\max,n} = (T_{\text{urban}} - T_{\text{reference}})_{\max,n} \text{ for nighttime} \quad (1)$$

Station numbered 2 is considered to be the reference station because it is nearly free from urban climate modifying effects, located at a less built-up area with low traffic and medium population.

The input parameters of the neural network models are the following:

- **Maximum daily values of the ambient air temperature** ($T_{\max}$ in °C), measured at each urban station: Maximum diurnal air temperature depends on various climatic factors such as the short-wave solar radiation, sunshine duration, vegetation and grounds' thermal properties, altitude and precipitation. Maximum diurnal air temperature values are significantly different in the urban environments because of the following reasons:
  - **a.** The reflectivity of a surface decreases as the surface irregularity increases.
  - **b.** Maximum air temperatures are higher in urban environments as a result of a smaller surface availability for evaporation. The release of anthropogenic heat from buildings and cars effects the significant increase of maximum diurnal air temperature.
  - **c.** Urban areas' geometry contributes to the trap of short-wave radiation in the urban canyons, thus increasing the energy absorption and resulting in higher maximum diurnal air temperatures.
  - **d.** Urban areas experience increased long-wave radiation because of higher temperature values, which are partly caused by the pollution that enhances the greenhouse effect.

Maximum daily air temperature is regarded as the representative urban parameter to the model, taking into account that it is the result of various major physical processes produced in the urban environment.

- **Nighttime values of the ambient air temperature** (T_{ref} in °C), measured at the reference station, at the time when $\Delta T_{\max,n}$ is observed: Nighttime air temperature at the reference station is an important parameter contributing significantly to the heat island intensity estimation. The reference temperature is usually lower than the corresponding urban temperature, especially during calm and clear nights. This is mainly caused by the stronger rural cooling rates if compared with those of the urban environments. That means that the city air cools at a slower rate. This difference can be explained by the following factors :
  - **a.** Building materials are characterized by relatively high thermal conductivity and volumetric heat capacity. Because of the high values of building materials'

thermal properties, daytime heat is able to both penetrate and be stored easily. At nighttime, as the surface temperature drops, the heat flux is directed upwards, thus helping to maintain relatively higher temperatures in the urban areas while the cooling rate is retarded.

b. Ground cooling is significantly delayed during clear and calm evenings in urban areas because of the surface geometry, which contributes to the obstruction of the cold night-sky in the canyons, thus decreasing the loss of the outgoing long-wave radiation. Moreover, the surface geometry aids decreasing wind velocity and turbulence in deep "city canyons," thus reducing the loss of sensible and latent heat.

c. The urban temperatures at night are higher than those of the surrounding environment due to the added heat of combustion.

These two input parameters are able to express the urban/surrounding countryside energy balance differences. The daily maximum air temperature is the result of the climatic conditions and the energy budget alterations at the urban environment while T_{ref} characterizes the surrounding countryside energy balance at nighttime, dominated mainly by the increased cooling rates.

The outputs of the neural network model are the nighttime heat island intensity values for each of the remaining twenty-two stations. Heat island intensity can be regarded as a measure of the numerous physical processes that produce the difference between rural and urban areas.

Training is performed using nighttime values of the input parameters for the heat island estimation of the heat island intensity for 550 days during 1996 and 1997 (one and a half years). As learning occurs, the mean square error decreases. The training results are compared with the measured heat island intensity values at each station. The comparison showed a good agreement between estimated and measured values for the entire set of experimental stations. Figure 3 displays the comparison of the measured heat island intensity values with the neural network estimated values for a set of six stations (numbers 3, 4, 12, 14, 15, 20), which are randomly selected for the presentation of results. In this figure x axis represents the measured urban heat island values, (°C), while y axis represents the estimated values in °C. As shown, there is a good agreement between measured and estimated values. The same good agreement is observed for the entire set of twenty-two stations. The correlation coefficients varied between 0.85 to 0.96, while the mean square errors fluctuated between 0.1 °C to 0.3 °C.

The temporal variation of the estimated and measured nighttime heat island intensity for four cases consisting of fifteen continual days of the training period (July 1996), and for four randomly selected stations (numbers 7, 9, 11, 18) is shown in Figure 4. In this figure the x axis represents time and its units are days, while the y axis represents heat island intensity and its units are °C. The solid line indicates the measured heat island values, while the plus symbols indicate the model estimations. As can be observed, there is a very good agreement between the estimated and the

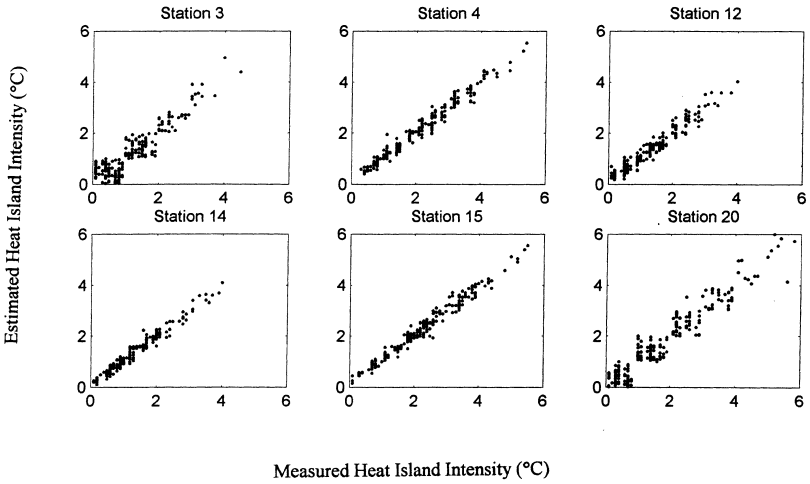

Figure 3
Comparison of the measured with the neural network estimated maximum nighttime heat island intensity values, for the training set of data and for six randomly selected experimental stations.

measured data. For these days, the 90% of the relative error (%RE) values fall between −15% and 10%.

$$(\%\mathrm{RE}) = [(\Delta T_{\max,n,\mathrm{meas}} - \Delta T_{\max,n,\mathrm{est}})/\Delta T_{\max,n,\mathrm{meas}}] * 100$$

where, $\Delta T_{\max,n,\mathrm{meas}}$ and $\Delta T_{\max,n,\mathrm{est}}$ are the measured and estimated nighttime heat island intensities, respectively.

From Figure 4 it can also be seen that the nighttime heat island intensity is higher, (reaching 5.4 °C), at the central densely populated and built station numbered 7, while at the other three stations it fluctuated between 0.5 and 3.5 °C. Similar performance is observed for the whole set of training data.

The accuracy of the neural network estimations is tested by comparing the measurements of the testing set of data, which consists of the nightly heat island intensity values for the remaining 180 days of 1997 (half a year), with the estimated results of the neural network approach. Figure 5 shows the comparison between the estimated heat island intensity values and the measured values for the testing set of data and for six randomly selected stations (numbers 4, 5, 8, 12, 13, 15). The results are quite encouraging for the complete set of twenty-two stations. The mean square errors varied between 0.2 °C to 0.3 °C while the correlation coefficients fluctuated between 0.80 to 0.92.

The temporal variation of the estimated nighttime heat island intensity values and of the testing set of measurements for fifteen continual days of the testing period (November 1997), and for four randomly selected stations (numbers 3, 12, 13, 17) is presented in Figure 6. The synoptic categories influencing the weather in the greater Athens area during this period are a high pressure ridge which enforces the

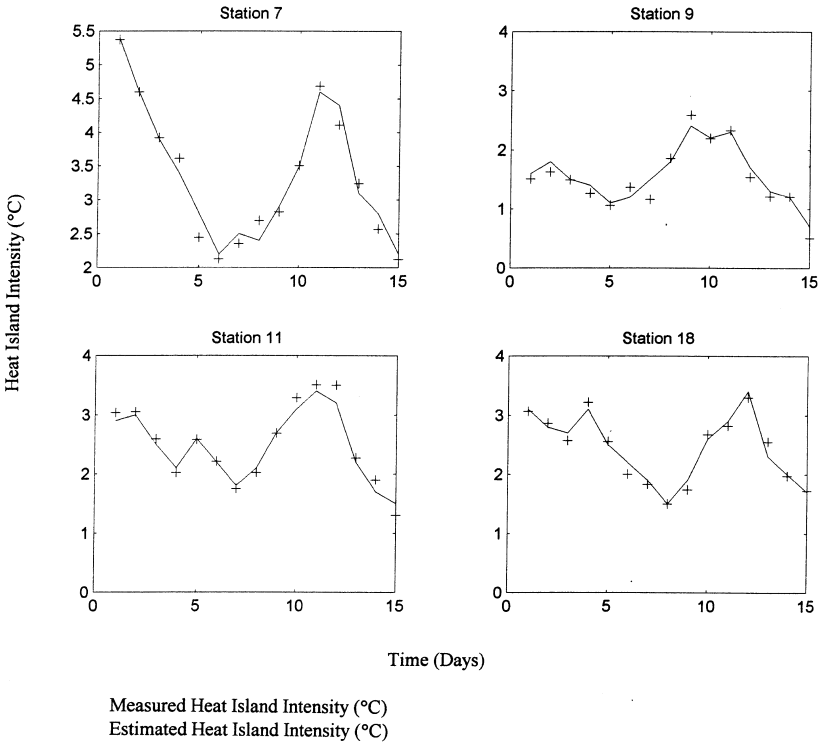

Figure 4
Temporal variation of the estimated and measured maximum nighttime heat island intensity values for fifteen continual days of the training period and for four randomly selected experimental stations.

development of the heat island effect and furthermore a southwesterly flow, characterized by strong winds which decrease the intensity of the phenomenon. From this figure one can observe a variation of the heat island intensity from night to night, which can be explained by the fact that November in the Athens area is a month predominated by a southwesterly flow circulation usually correlated with surface cyclonic patterns and baroclinic instability. The main characteristic of this flow pattern is that the winds blowing from the southern sector sustain medium to strong intensity (more than 6 m/sec), influencing in this way the urban climatic conditions and enhancing the large fluctuations of the heat island intensity. From this figure it can also be seen that the neural network estimations perform well on the testing set of measurements. Similar performance is observed for the entire testing set.

3.2. Results and Discussion

Neural network models are used to investigate and analyze the impact of the two input climatic parameters on the fluctuation of the heat island intensity during

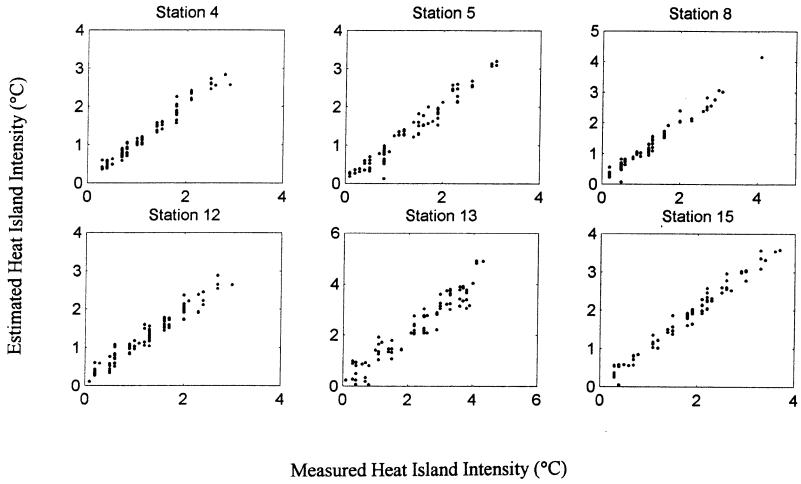

Figure 5
Comparison of the measured with the neural network estimated maximum nighttime heat island intensity values, for the testing set of data and for six randomly selected experimental stations.

nighttime. For this investigation, neural networks are designed and trained for the nighttime heat island estimation using only one parameter as input each time, for ten randomly selected stations and for the same time period. The models' results are summarized in Table 2 where one can see the correlation coefficients between the measured and estimated maximum heat island intensity values for the following three cases:

- When both parameters, (T_{max}, and T_{ref}), are used as inputs to the neural network models. In this case the correlation coefficient is represented by λ_1.
- When daily maximum ambient air temperature, (T_{max}), is the only input parameter. In this case the correlation coefficient is represented by λ_2.
- When T_{ref} is the only input parameter. In this final case the correlation coefficient is represented by λ_3.

All correlation coefficients are calculated on the training set of data. Table 2 shows that the use of one parameter as input to the models results in a remarkable reduction of the correlation coefficient which can be described as follows:

- For the use of maximum air temperature as input parameter representing the prevailing climatic conditions at each urban station, the correlation coefficient decrease varied between 18 and 27%.
- For the use of T_{ref} as input parameter representing the energy balance at the reference station, the correlation coefficient reduction fluctuated between 24 and 35%.

The above results demonstrate that the agreement between estimated and measured values of the nighttime heat island intensity is slightly better when the daily maximum air temperature is used as the unique input to neural models. This can be explained by the fact that the daily maximum air temperature is more representative

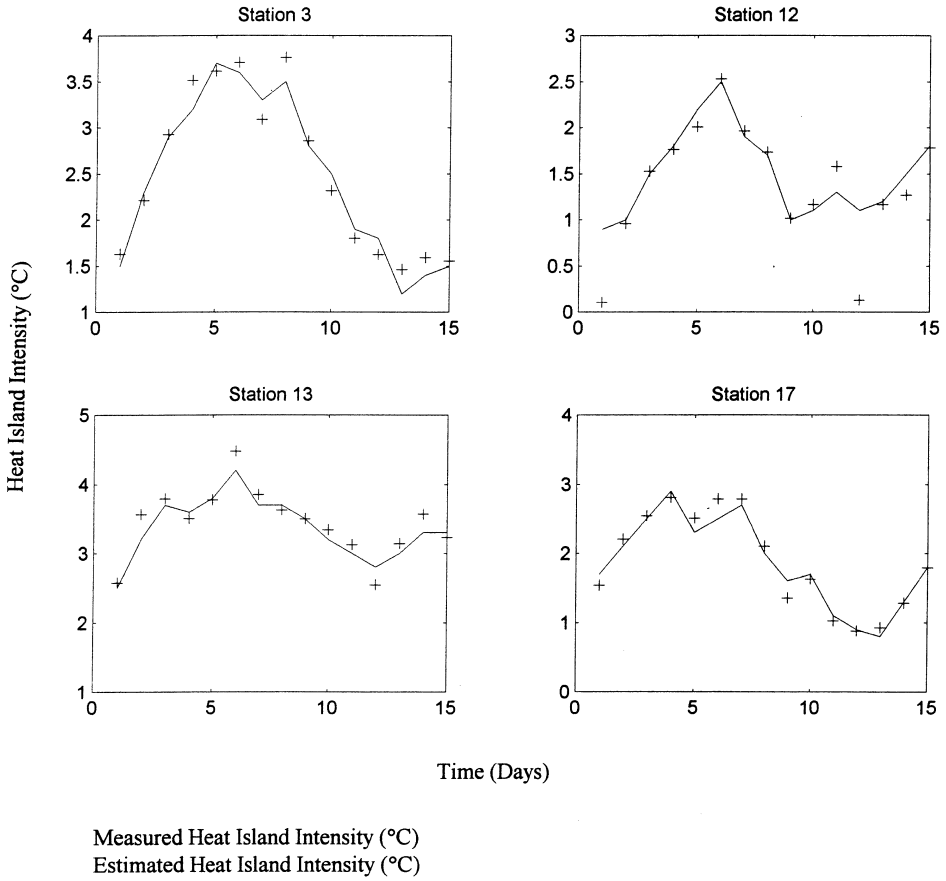

Figure 6
Temporal variation of the estimated maximum nighttime heat island intensity values and of the testing set of measurements for fifteen continual days of the testing period and for four randomly selected experimental stations.

of the urban environment physical processes producing the heat island phenomenon as it is measured at all urban stations. Conversely, nighttime reference temperature is the result of only the surrounding countryside climatic conditions.

However, the use of both climatic parameters improves drastically the results as they complement the urbanization process description, offering a more integral and representative illustration of the difference between urban/surrounding countryside. The maximum daily air temperature contributes to the presentation of the urban environmental conditions while the T_{ref} is responsible for the surrounding countryside thermal balance. Therefore, the two parameters as inputs to the neural models are able to produce the urban/surrounding countryside energy balance differences, which result in the urban heat island effect.

Table 2

*Correlation coefficients between the measured and neural networks estimated nighttime heat island intensity values for the three considered cases of T_{max}, and T_{ref} as inputs to the neural networ*k (λ_1), *of T_{max}, as the only input parameter (λ_2), and of T_{ref} as the only input parameter (λ_3)*

Station	λ_1	λ_2	(%) Reduction	λ_3	(%) Reduction
1	0.89	0.65	27.0	0.58	34.8
4	0.91	0.67	26.4	0.63	30.8
6	0.93	0.69	25.8	0.66	29.0
7	0.93	0.68	26.9	0.65	30.1
11	0.94	0.69	26.6	0.66	29.8
12	0.95	0.78	17.9	0.72	24.2
13	0.94	0.69	26.6	0.67	28.7
15	0.90	0.66	26.6	0.64	28.9
16	0.86	0.70	18.6	0.63	26.7
17	0.90	0.66	26.7	0.61	32.2
19	0.91	0.66	27.5	0.64	29.7
20	0.94	0.69	26.6	0.67	28.7

4. Fluctuations of the Daytime Heat Island Intensity

4.1. Modeling the Daytime Heat Island Intensity

The fluctuations of daytime heat island intensity are also estimated using neural network models.

In this case, multiple feed-forward networks based also on a backpropagation method are designed to learn and then estimate the daytime heat island intensity. Neural network models are built separately for each one of the experimental stations. The architecture of the network, which is selected after trying several networks, includes one hidden layer of 18 to 22 log-sigmoid neurons followed by an output layer of one linear neuron.

Again, the network is trained over a certain part of the climatic data and furthermore, the network's ability is tested using the remaining data. The training and testing data are the measurements taken from the experimental stations presented and described in section 2. The neural models are designed and trained for the estimation of the stations heat island intensity, ($\Delta T_{max,d}$ in °C) during the daytime and for the same time period.

$$\Delta T_{max,d} = (T_{urban} - T_{reference})_{max,d} \text{ for daytime} \quad (2)$$

The neural networks output is the heat island intensity at daytime and for the twenty-two stations. At this case, the selected input parameters of the models are:

- **Daytime values of ambient air temperature**, (T_{air}, in °C), measured at each urban station at the time when the $\Delta T_{max,d}$ is observed: The daytime temperature

values at the urban stations can be regarded as the result of all natural processes produced by the urbanization during the day as analyzed in section 3.

- **Maximum daily values of global solar radiation**, (I_g, in MJ/m^2), measured at the radiometric station of the National Observatory of Athens (NOA, station numbered 1): The measured values of global solar radiation at station 1 are used as representative of short-wave solar radiation and sunshine.
- **Daytime values of reference air temperature**, (T_{ref}, in °C), measured at the reference station at the time when the $\Delta T_{\max,d}$ is observed: The daytime reference temperatures represent the energy balance at the reference station, which is regarded as representative of the surrounding countryside climatic conditions.

Training is performed using daily values of the input parameters for the same time period as in section 3. The estimated results are compared with the measured daytime heat island intensity values at each station. From the comparison it is observed that the estimated values perform well with the measured ones. Twelve randomly selected stations (numbers 1, 5, 7, 8, 9, 10, 11, 12, 14, 15, 18, 20), are used for the presentation of the training results (Fig. 7). As shown, there is a good agreement between the measured and estimated values. Similar agreement is observed for the whole set of the twenty-two stations. The correlation coefficients fluctuated between 0.85 to 0.97 while the mean square errors varied 0.1 °C to 0.3 °C. The urban stations, which are characterized by heavy traffic, increased air pollution, and buildings' density, present the better estimations. In these stations (numbers 3, 7, 9, 11, 12, 13, 15, 18, 20, 21, 23) the correlation coefficient fluctuated between 0.90 to 0.97. For the remaining stations, which are influenced by several topographic and synoptic conditions such as local flows like the sea breeze of Saronikos gulf (numbers 6, and 10), katabatic flows from the mountains (numbers 1, 5 and 8), high vegetation (numbers 14, 16, 19 and 22), low traffic and building density (numbers 4 and 17), the correlation coefficients varied between 0.83 to 0.92.

The temporal variation of the estimated and measured daytime heat island intensity for four cases of fifteen continual days of the training period (August 1996), and for four randomly selected stations (numbers 8, 10, 12, 23) is shown in Figure 8. The summer period over the Athens area is dominated by anticyclonic circulation in the lower troposphere, consistent with the increase of the anticyclonic tracks and the corresponding decrease of cyclonic tracks over the central and eastern Mediterranean (MAKROGIANNIS and GILES, 1980). This weather situation favors strongly the increase of diurnal heat island intensity, which as shown in Figure 8 is significantly high especially for station 12, where it rises to 15.4 °C. Station 12 is regarded as the most representative of strong urban conditions. Moreover, from this figure, it can be seen that the estimated values perform well on the measured data. Similar performance is observed for the whole set of training data.

Furthermore, and in order to check the accuracy of the neural network estimations, the measurements of the testing set of data, which remain the same as in section 3, are compared with the neural estimations. Figure 9 illustrates the

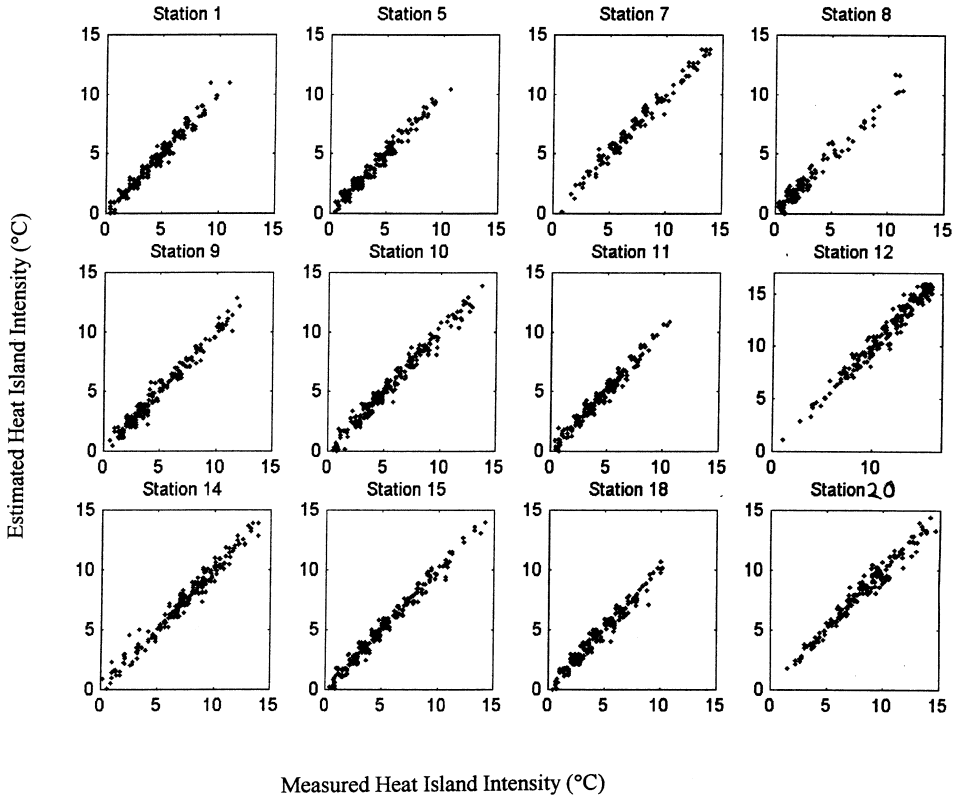

Figure 7
Comparison of the measured with the neural network estimated maximum daytime heat island intensity values for the training set of data and for twelve randomly selected experimental stations.

comparison between the estimated and measured values of the testing set of data for six randomly selected stations (numbers 7, 8, 12, 15, 18, 20). The results validate the good agreement for the entire set of the twenty-two stations. The correlation coefficients fluctuated between 0.80 to 0.94 while the mean square errors varied in the range of 0.2 °C to 0.4 °C.

4.2. Results and Discussion

The heat island intensity is not a constant condition. It shows both periodic and non-periodic fluctuations depending on weather conditions as well as on topographic and topoclimatic complexities and synoptic flow patterns. Table 3 shows the mean seasonal heat island intensity at daytime for the twenty-two stations and for a two-year time period (1996–1997), using station 2 as reference station. As shown, the mean seasonal daytime heat island intensity values for the seven central stations are reported as follows: 7.5 °C for summer, 5.1 °C for autumn, 3.7 °C for winter, and

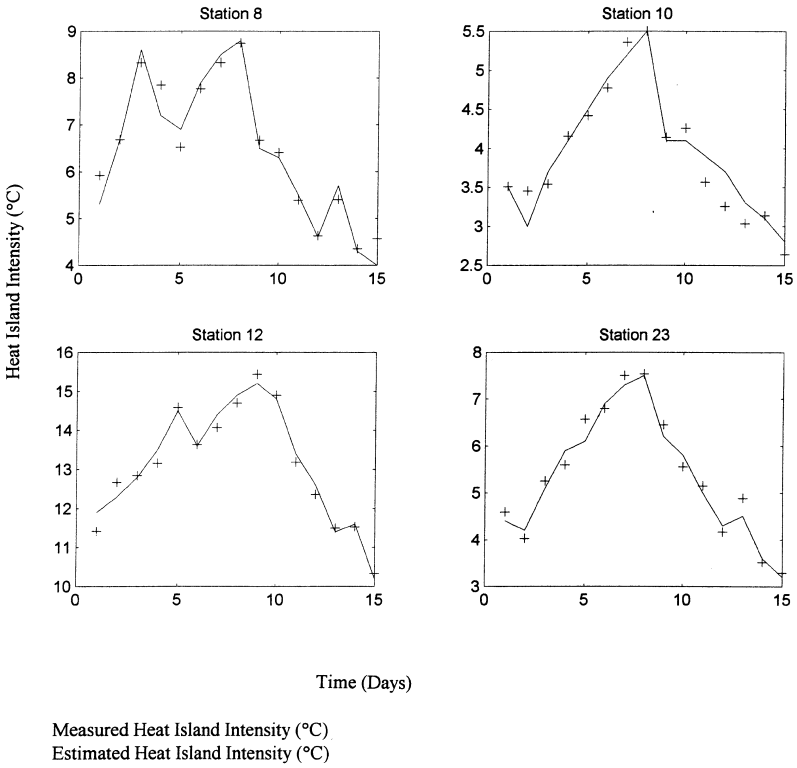

Figure 8
Temporal variation of the estimated and measured maximum daytime heat island intensity values for fifteen continual days of the training period and for four randomly selected experimental stations.

4.6 °C for spring. Accordingly, the mean seasonal values for the fifteen urban stations around Athens are: 5.4 °C for summer, 3.2 °C for autumn, 2.1 °C for winter, and 3.1 °C for spring.

The impact of the three main input climatic parameters on the fluctuation of the heat island intensity during daytime is further investigated. Therefore, one parameter is used as input to the neural models at each time for ten randomly selected stations and for the same time period. The models' results are presented in Table 4, which presents the correlation coefficients between the measured and estimated daytime heat island intensity values. The results are analyzed as follows:

- The correlation coefficient, (λ_4), is used for the presentation of results when the three parameters, (T_{air}, I_g, and T_{ref}), are used as inputs to the neural network models.
- The correlation coefficient, (λ_5), is used for the presentation of results when the daytime values of ambient air temperature, (T_{air}), are the only input parameter.

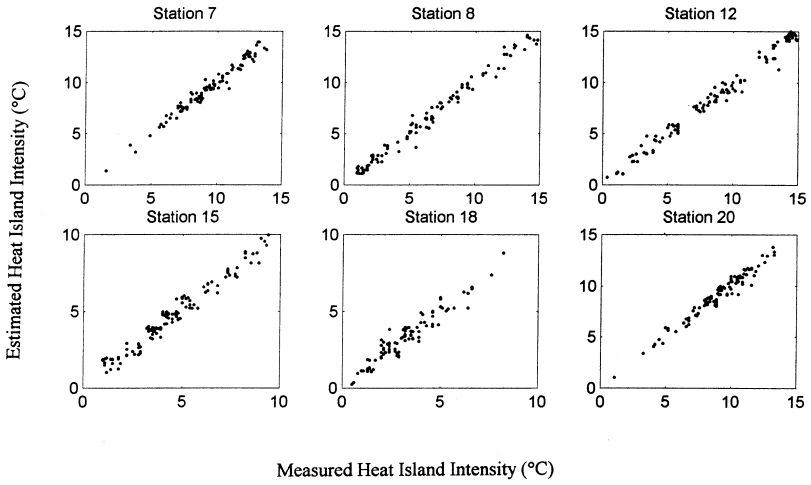

Figure 9
Comparison of the measured with the neural network estimated maximum daytime heat island intensity values for the testing set of data and for six randomly selected experimental stations.

Table 3

Mean seasonal heat island intensity at daytime for the twenty-two stations and for two-year time period (1996–1997), using station 2 as rural station.

Station	$D\Delta T_{max}$ for Summer (°C)	$D\Delta T_{max}$ for Autumn (°C)	$D\Delta T_{max}$ for Winter (°C)	$D\Delta T_{max}$ for Spring (°C)
1	5.2	3.4	2.6	3.6
3	6.3	4.2	2.9	4.7
4	5.9	3.4	1.9	3.1
5	6.6	3.7	2.2	2.8
6	3.2	2.4	1.1	2.0
7	8.2	5.1	4.9	5.7
8	5.2	2.8	1.6	3.3
9	7.9	3.8	2.8	4.3
10	8.3	4.4	2.8	5.2
11	5.2	3.5	3.1	3.0
12	9.7	7.2	5.9	6.1
13	8.6	6.1	5.2	5.9
14	7.1	5.3	3.9	4.9
15	8.2	5.9	1.9	5.0
16	2.6	1.1	0.8	1.7
17	6.6	4.2	2.7	3.1
18	5.6	3.8	2.2	3.4
19	1.5	0.7	0.4	0.8
20	7.2	4.8	3.1	4.3
21	3.9	2.7	1.8	2.5
22	5.2	3.3	2.1	2.2
23	4.8	2.6	1.9	2.5

Table 4

Correlation coefficients between the measured and neural networks estimated daytime heat island intensity values for the four considered cases of the three parameters, (T_{air}, I_g, and T_{ref}), used as inputs to the neural network models (λ_4), of T_{air} as the only input parameter (λ_5), of global solar radiation, (I_g), as the only input parameter (λ_6) and of T_{ref} as the only input parameter (λ_7)

Station	λ_4	λ_5	(%) Reduction	λ_6	(%) Reduction	λ_7	(%) Reduction
1	0.89	0.61	31.5	0.52	41.6	0.55	38.2
7	0.96	0.69	28.1	0.60	37.5	0.63	34.4
8	0.94	0.69	26.6	0.59	37.2	0.57	39.4
10	0.88	0.65	26.1	0.53	39.8	0.59	33.0
11	0.90	0.68	24.4	0.54	40.0	0.60	33.3
12	0.95	0.68	28.4	0.56	41.1	0.59	37.9
14	0.95	0.70	26.3	0.55	42.1	0.62	34.7
15	0.92	0.66	28.3	0.55	40.2	0.61	33.7
18	0.89	0.64	28.1	0.52	41.6	0.56	37.1
23	0.85	0.61	28.2	0.49	42.4	0.53	37.6

- The correlation coefficient, (λ_6), is used for the presentation of results when global solar radiation, (I_g), is the only input parameter.
- The correlation coefficient, (λ_7), is used for the presentation of results when reference temperature (T_{ref}) is the only input parameter.

All correlation coefficients are calculated on the training set of data. As can be seen from Table 4, the use of the three input parameters improves significantly the correlation between the measured and estimated values. This can be explained by the fact that the neural model is enriched by a multitude of input parameters describing both urban and rural climatic conditions and representing the most significant energy balance processes which govern the creation of the heat island phenomenon. However, the use of one parameter as input to the models results in a remarkable reduction of the correlation coefficient which can be described as follows:

- For the use of daytime ambient air temperature as a single input parameter representing the prevailing climatic conditions at each urban station, the reduction of correlation coefficient varied between 24 and 31%.
- For the use of global solar radiation as a single input parameter representing the highest part of the incoming energy at daytime, the reduction of correlation coefficient varied between 37 and 42%.
- For the use of reference temperature as a single input parameter, which is the result of the prevailing climatic conditions at the reference station, the correlation coefficient decrease fluctuated between 33 and 39%.

The above results demonstrate that the agreement between estimated and measured values of the daytime heat island intensity is significantly better when the daytime air temperature at each urban station is used as the unique input to neural models. This can be explained by the fact that heat island intensity at each urban station is mainly dominated by the thermal balance processes developed at each

station. The daytime temperature measured at the urban locations is the result of various candidate causes, analytically described in the previous section, considered responsible for the relative warmth of the air of cities. For this reason T_{air} is the most crucial input parameter. T_{ref} expresses the thermal balance status at the reference station and has a significant impact on the heat island estimation as it is the result of a number of energy and climatic factors prevailing at the reference station area. Finally, global solar radiation is shown from the present research as the less powerful from the three input parameters. This can be expected as T_{air} and T_{ref} are the results of all climatic factors including the short-wave solar radiation which partly causes the heat island phenomenon. Moreover, the values of global solar radiation are those measured at the station numbered 1 surface and are used for all stations. This is not thoroughly accurate as the amount of the arriving short-wave radiation at the surface of each station depends on urban atmospheric conditions (pollution).

5. Conclusions

The nighttime and daytime values of urban heat island intensity in twenty-three stations located in the Athens' major area and for a two-year time period, were estimated using neural network systems.

For the nighttime estimations, two climatic parameters were used as inputs to the models: the maximum daily air temperature measured at each urban station and a reference temperature measured at the considered surrounding countryside station. The simulated results can be outlined as follows:

1. The use of daily maximum air temperature measured at each urban station as a single input parameter to the neural models produced a decrease of the correlation coefficient which fluctuated between 18 and 27%.
2. The use of reference temperature as the only input to the neural models resulted in a higher reduction of correlation coefficient between measured and estimated values which varied between 24 and 35%.
3. The observed agreement between estimated nighttime heat island intensity and measured ones is quite good for both training and testing sets of measurement.

As regards the daytime estimations, the three climatic parameters used as inputs to the models were: The daytime air temperature measured at each urban station, the global solar radiation and the reference temperature measured at the reference station. The results can be summarized as follows:

1. The daytime air temperature as a single input parameter caused a reduction of correlation coefficient with varied between 24 and 31%.
2. The global solar radiation, as the only input parameter, created a significant decrease of the correlation coefficient between measured and estimated values which have risen up to 42%.

3. The reference temperature as a single input parameter produced a reduction of the correlation coefficient which fluctuated between 33 and 39%.
4. The estimated diurnal heat island intensity values perform well with the measured ones for both training and testing sets of measurement.

Therefore, for the nighttime and daytime estimations, the urban air temperature, representing the energy balance processes at each station, is the predominant input parameter, thus emphasizing the importance of the urban climatic conditions on the heat island phenomenon. The heat island intensity is a meteorological element dependent on the background climate and the prevailing synoptic scale meteorological conditions, the effects of the local landscape and the effects of local urbanization.

References

Asimakopoulos, D. N., Deligiorgi, D. G., Drakopoulos, C., Helmis, C., Kokkori, K., Lalas, D. P., Sikiotis, D., and Varotsos, C. (1992), *An Experimental Study of Nighttime Air-pollutant Transport over Complex Terrain in Athens*, Atmos. Environ. *B 26*, 59–71.

Barring, L., Mattsson, J. O., and Lindqvist, S. (1985), *Canyon Geometry, Street Temperatures and Urban Heat Island in Malmo*, Sweden, J. of Climatology *5*, 433–444.

Chakraborty, K., Mehrotra, K., Mohan, C. K., and Ranka, S. (1992), *Forecasting the Behavior of Multivariate Time Series Using Neural Networks*, Neural Networks *5*, 961–970.

Cichocki, A. and Unbehauen, R., *Neural Networks for Optimization and Signal Processing* (John Wiley & Sons, Stuttgart, Germany 1993).

Dash, P. K., Ramakrishna, G., Liew, A. C., and Rahman, S. (1995), *Fuzzy Neural Networks for Time-series Forecasting of Electric Load*, IEE Proc.-Gener. Transm. Distrib. *142*, 535–544.

Eliasson I. (1996) *Urban Nocturnal Temperatures*, *Street Geometry and Land Use*, Atmos. Environ. *30*, 379–392.

Escourrou, G. (1991), *Climate and Pollution in Paris*, Energy and Buildings, *15–16*, 673–676.

Givoni, B. (1989), *Urban Design in Different Climates*, WMO Technical Report 346.

Helmis, C. G., Asimakopoulos, D. N., Papadopoulos, K. H., Kassomenos, P., Kalogiros, J. A., Papageorgas, P. G., and Blikas, S. (1997), *Air mass exchange between the Athens Basin and the Messogia Plain of Attika*, *Greece*, Atmos. Environ. *31*, 3833–3849.

Hondou, T. and Sawada, Y. (1994), *Analysis of Learning Processes of Chaotic Time Series by Neural Networks*, J. Prog. Theor. Phys. *91*, 397–402.

Johnson, G. T., Oke, T. R., Lyons, T. J., Steyn, D., Watson, I. D., and Voogt, I. D. (1991), *Simulation of Surface Urban Heat Islands under "Ideal" Conditions at Night - Part I: Theory and Tests against Field Data*, Bound.-Layer Meteor. *56*, 275–294.

Kalogirou, S., Neocleous, C., Michaelides, S., and Schizas, C. (1997), *A Time Series Reconstruction of Precipitation Records Using Artificial Neural Networks*, Proc. EUFIT'97, Aachen, Germany, 2409–2413.

Kassomenos, P., Flocas, H. A., Lykoudis, S., and Petrakis, M. (1998), *Analysis of Mesoscale Patterns in Relation to Synoptic Conditions over an Urban Mediterranean Basin*, Theor. Appl. Climatol. *59*, 215–229.

Landsberg, H. E., *The Urban Climate* (Academic Press. New York 1981).

Li, M., Mehrotra, K., Mohan, C. K., and Ranka, S. (1990), *Sunspot Numbers Forecasting Using Neural Networks*, Proc. IEEE Symp. Intelligent Control *1*, 524–529.

Lyall, I. T. (1997), *The London Heat Island in June–July 1976*, Weather *32*, 296–302.

Makrogiannis, T. J. and Giles, B. D. (1980), *Frequencies, Individual, and Mean Tracks of Moving Anticyclones over Southeast Europe*, J. Meteorol. *5*, 240–248.

MIHALAKAKOU, G., SANTAMOURIS, M., and ASIMAKOPOULOS, D. (1998), *Modeling the Ambient Air Temperature Time Series Using Neural Networks*, J. Geophys. Res. *103*, 19,509–19,517.

MIHALAKAKOU, G., FLOCAS, E., SANTAMOURIS, M., and HELMIS, C. (2001), *Application of Neural Networks to the Simulation of the Heat Island over Athens, Using Synoptic Types as a Predicto*, J. Appl. Meteorol. *41*, 519–527.

MONTAVEZ, J. P., RODRIGUEZ A., and JIMENEZ, J. I. (2000), *A Study of the Urban Heat Island of Granada*, Int. J. Climatol. *20*, 899–911.

MORRIS, C. J. G. and SIMMONDS, I. (2000), *Associations between Varying Magnitudes of the Urban Heat Island and the Synoptic Climatology in Melbourne, Australia*, Int. J. Climatol. *20*, 1931–1954.

OKE, T. R., *Boundary Layer Climates*, 2nd edition, Routledge (London and New York 1987).

OKE, T. R., JOHNSON, D. G., STEYN, D. G., and WATSON, I. D. (1991), *Simulation of Surface Urban Heat Island Under 'Ideal' Conditions at Night – Part 2: Diagnosis and Causation*, Bound.-Layer Meteor. *56*, 339–358.

PARK, H. S. (1986), *Features of the Heat Island in Seoul and its Surrounding Cities*, Atmos. Environ. *20*, 1859–1866.

PHAM, D. T. and LIU, X., *Neural Networks for Identification, Prediction and Control* (Springer-Verlag, Berlin 1995).

ROSENBLATT, F., *Principles of Neurodynamic* (Spartan Press, Washington, D.C. 1961).

RUMELHART, D. E., HINTON, G. E., and WILLIAMS, R. J. (1986), *Learning internal representations by error propagation*. In *Parallel Distributed Processing*, (eds. Rumelhart D.E. and McClelland J.L.) (MIT Press, Cambridge, Mass.) pp. 318–362.

SANTAMOURIS, M., MIHALAKAKOU, G., PAPANIKOLAOU, N., and ASIMAKOPOULOS, D. N. (1999a), *A Neural Network Approach for Modeling the Heat Island Phenomenon in Urban Areas during the Summer Period*, Geophys. Res. Lett. *26*, 337–340.

SANTAMOURIS, M., MIHALAKAKOU, G., PSILOGLOU, B., EFTAXIAS, G., and ASIMAKOPOULOS, D. N. (1999b), *Modeling the Global Solar Radiation on the Earth Surface Using Atmospheric, Deterministic and Intelligent Data Driven Techniques*, J. of Climate *12*, 3105–3116.

SANTAMOURIS, M., PAPANIKOLAOU, N., LIVADA, I., KORONAKIS, I., GEORGAKIS, C., ARGIRIOU, A., and ASIMAKOPOULOS, D. N. (2001), *On the Impact of Urban Climate on the Energy Consumption of Buildings*, Solar Energy *70*, 201–216.

SANTAMOURIS, M., *Energy and Climate in the Urban Built Environment* (James and James, London 2001).

(Received December 28, 2001, accepted January 17, 2003)